How do phase-change materials crystallize so fast?

In phase-change (PC) materials, a laser-induced rapid transformation to the crystalline phase can occur within tens of nanoseconds, and their amorphous phases are stable at room temperature (RT) for several decades. Until today, two classes of materials, namely, GeTe–Sb_2Te_3 pseudobinary compounds (group 1 in Fig. 1(a)) and Sb–Te binary compounds with small amounts of In, Ag and/or Ge (group 2 in Fig. 1(a)) have been practically completed and used extensively in rewritable high-density optical disks such as DVDs and Blu-ray Discs™. Furthermore, non-volatile electric solid-state memory called PC-RAM (random access memory) has also been launched in the market in recent years [1]. However, the accurate PC mechanism has remained the subject of speculations despite their brilliant commercial successes. For example, it is well-known that crystallization processes are strikingly different between the two groups of materials, as shown in Fig. 1(b). Nevertheless, the origin of the difference has not been systematically explained at the atomistic level, yet. Since crystallization is the rate-limiting process in all PC devices, an atomistic understanding of the difference is essentially important for obtaining next-generation PC alloys.

Such a delay in understanding the mechanism is caused by the lack of structure information of amorphous materials. To solve the situation, our research group has constructed an “X-ray pinpoint structural measurement system” at SPring-8 that enabled us to perform real-time and high-quality observation of nanoscaled structure change from the amorphous phase to the crystalline phase [2]. Using the system, we found that the crystallization processes were very different on the nanosecond order at the atomistic level between GST and AIST, and succeeded in finding NaCl-like fragments as nuclei in amorphous $Ge_2Sb_2Te_5$ [3]. Furthermore, we proposed an effective method of analyzing the structure of amorphous materials. We combined density functional (DF)-molecular dynamics (MD) and reverse Monte Carlo (RMC) simulations for amorphous GST (a-GST) and successfully reproduced using the obtained simulation the experimental data of X-ray diffraction (XRD) and hard X-ray photoelectron spectroscopy (HXPS) [4].

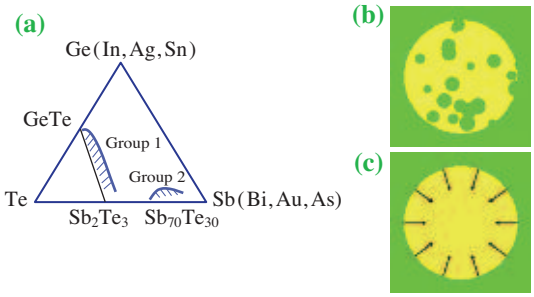

Fig. 1. Phase diagram of typical PC materials and crystallization patterns. **(a)** The most commonly used materials for optical recording are groups 1 and 2. **(b)** Nucleation-dominated recrystallization (as in GST). **(c)** Growth-dominated recrystallization (AIST).

In the present study, we applied several techniques (XRD experiment, HXPS and extended X-ray absorption fine structure (EXAFS) combined with DF-MD simulations) to determine the amorphous and crystalline structures of the AIST alloy $Ag_{3.5}In_{3.8}Sb_{75.0}Te_{17.7}$ (AIST). Consequently, we found distinct differences between the structures of GST (group 1) and AIST (group 2), which have wider implications. The experiments were carried out at beamlines **BL04B2**, **BL14B2**, and **BL47XU**.

Figure 2 shows the XRD data for AIST (Fig. 2(a)) together with that for GST (Fig. 2(b)), and their atomistic configurations obtained by DF-RMC simulation. These results show that the calculated structure finely agrees with experimental results including XRD data and HXPS measurements of the electronic structure (not shown here). The structural difference between a-AIST and a-GST is clearly visible in Figs. 2(c) and 2(d) [5]. Amorphous AIST has a highly random network structure whose ring statistics range widely, whereas a-GST has many small rings with ‘AB alternation’ (A=Ge or Sb; B=Te) that act as nuclei in the (nucleation-driven) crystallization process involving large fraction of cavities.

Then, a rough image of a-AIST is obtained. The next step is analyzing the detailed local structure. It is natural that an understanding of the rapid crystallization mechanism will be gained by comparing the bonding and atomic distributions in a-AIST and c-AIST. The principal information obtained through this study is as follows: (i) Crystalline AIST (c-AIST) has short (2.93 Å) and long (3.30 Å) bonds, while a-AIST has the shortest bond of 2.86 Å with a shoulder at 3.5 Å. (ii) The bond angle distribution in a-AIST is very similar to that in c-AIST; the maximum bond angle for short bonds (<3.1 Å) of a-AIST is 95 degrees as in c-AIST as though the distribution range of a-AIST is wider than that of c-AIST. (iii) The chemical coordination numbers N_{bond} of Ag , Sb and Te in a-AIST are almost the same as those in c-AIST; for instance, the N_{bond} values for Sb are 3.1 in a-AIST and 3.2 in c-AIST. (iv) The profiles of the bond order (the number of chemical bonds between two atoms) are very similar in both phases for each kind of bond and

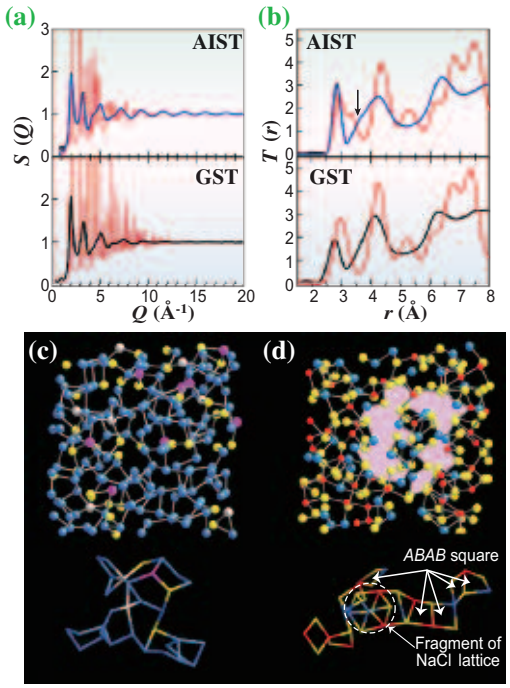

Fig. 2. HXRD data for AIST and GST, and atomic configurations of a-AIST and a-GST. **(a, b)** Structure factors *S(Q)* and total correlation functions *T(r)* of AIST and GST (Ref. 4). Red line, experimental data of crystalline phase; black line, experimental data of amorphous phase; blue line, DF-RMC model of a-AIST. The DF-RMC and experimental results are practically indistinguishable. **(c)** Section of 640-atom DF-MD model of a-AIST (24 Å_24Å_12 Å). Ag, silver; In, magenta; Sb, blue; Te, yellow. **(d)** Section of 460-atom DF-MD model of a-GST (24 Å_24Å_12 Å). Ge, red; Sb, blue; Te, yellow; large cavity, pink.

the value is less than unity everywhere, showing that both phases are not perfectly covalent. (v) The main peak of the bond-order profile in c-AIST is located at 0.67 and that in a-AIST is located at 0.75, suggesting that a-AIST is more covalent than c-AIST.

With this information, we reached an understanding of the local environment around Sb atoms (main component) and drew a picture of the rapid crystallization process of a-AIST.

As shown in Fig. 3, both a-AIST (upper left in Fig. 3) and c-AIST (upper right in Fig. 3) resemble a distorted 3+3 octahedron. The bonds in a-AIST are slightly shorter (stronger) than those in c-AIST, with enhanced insulating or semiconducting features; however, c-AIST has a Jahn-Teller distorted octahedral structure (nearly simple cubic) and more metallic features. When the bond electrons in a-AIST are excited by laser light or electric stimulation, the center atom with three short (red) and three long (dashed) bonds slightly moves and eventually changes its position to the center of the octahedron with a bond interchange between short (strong) and long (weak) bonds. The resultant resonant bonding produced between periodic short and long bonds leads to a crystalline A7 network. This is just the beginning of the rapid PC in group 2, including AIST. Each vector in the lower figures defines the direction of the corresponding distorted octahedron. In the recording marks of a-AIST, the direction of the vector is random (lower left in Fig. 3), and laser irradiation or electric heating can lead to a sequence of small atomic shifts that align the vectors along the c-axes of crystalline (A7, hexagonal) cells in the rim; therefore, the entire amorphous mark assume the A7 structure (lower right in Fig. 3). This is the origin of the 'growth-dominated' crystallization in group 2. In contrast, there are many fragments of the NaCl lattice in a-GST as previously reported, and crystallization starts simultaneously from many such nuclei in the amorphous mark ('nucleation-dominated' crystallization).

It cannot be denied that our model has some speculations. We hope to clarify more details of its mechanism through our future works and to create novel PC materials suitable for the ultrahigh-density storage media in the near future.

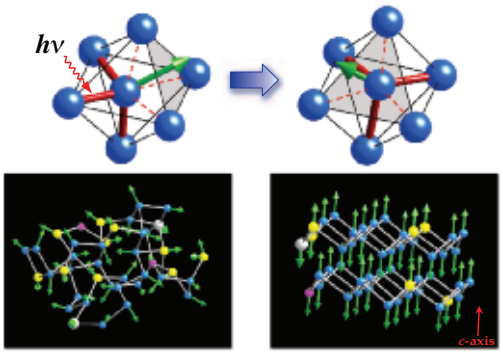

Fig. 3. PC mechanism of a-AIST.

Noboru Yamada[a,d,*], Toshiyuki Matsunaga[b,d] and Masaki Takata[c,d]

[a] Digital Network Technology Development Center, Panasonic Corporation
[b] Materials Science and Analysis Technology Center, Panasonic Corporation
[c] SPring-8 / RIKEN·JASRI
[d] CREST

* E-mail: yamada.noboru@jp.panasopnic.com

References

[1] M. Wuttig and N. Yamada: Nature Mater. **6** (207) 824.
[2] S. Kohara *et al.*: Appl. Phys. Lett. **89** (2006) 201910.
[3] Y. Fukuyama *et al.*: Appl. Phys. Exp. **1** (2008) 045001.
[4] J. Akola *et al.*: Phys. Rev. B **80** (2009) 020201.
[5] *T. Matsunaga, J. Akola, S. Kohara, T. Honma, K. Kobayashi, E. Ikenaga, R.O. Jones, N. Yamada, M. Takata and R. Kojima: Nature Mater.* ***10*** *(2011)129.*